



UNIVERSITY OF LEEDS

This is a repository copy of *The Unprecedented Ozone Loss in the Arctic Winter and Spring of 2010/2011 and 2019/2020*.

White Rose Research Online URL for this paper:

<https://eprints.whiterose.ac.uk/196401/>

Version: Accepted Version

Article:

Ardra, D, Kuttippurath, J, Roy, R et al. (4 more authors) (2022) The Unprecedented Ozone Loss in the Arctic Winter and Spring of 2010/2011 and 2019/2020. ACS Earth and Space Chemistry, 6 (3). pp. 683-693. ISSN 2472-3452

<https://doi.org/10.1021/acsearthspacechem.1c00333>

© 2022 American Chemical Society. This is an author produced version of an article published in ACS Earth and Space Chemistry. Uploaded in accordance with the publisher's self-archiving policy.

Reuse

Items deposited in White Rose Research Online are protected by copyright, with all rights reserved unless indicated otherwise. They may be downloaded and/or printed for private study, or other acts as permitted by national copyright laws. The publisher or other rights holders may allow further reproduction and re-use of the full text version. This is indicated by the licence information on the White Rose Research Online record for the item.

Takedown

If you consider content in White Rose Research Online to be in breach of UK law, please notify us by emailing eprints@whiterose.ac.uk including the URL of the record and the reason for the withdrawal request.



eprints@whiterose.ac.uk
<https://eprints.whiterose.ac.uk/>

1 The unprecedented ozone loss in the Arctic winter and spring of
2 2010/2011 and 2019/2020

3 Divakaran Ardra^{1,2}, Jayanarayanan Kuttippurath^{1,*}, Raina Roy^{1,2}, Pankaj Kumar¹, Sarath Raj¹, Rolf Müller³ and
4 Wuhu Feng^{4,5}

5 ¹*CORAL, Indian Institute of Technology Kharagpur, Kharagpur, 721302, India*

6 ²*Department of Physical Oceanography, Cochin University of Science and Technology, Kochi.*

7 ³*Forschungszentrum Jülich GmbH (IEK-7), 52425 Jülich, Germany*

8 ⁴*National Centre for Atmospheric Science, University of Leeds, Leeds, LS2 9PH, UK*

9 ⁵*School of Earth and Environment, University of Leeds, Leeds, LS2 9JT, UK*

10 *Corresponding author: jayan@coral.iitkgp.ac.in

11

12

13

14

15

16

17

18 HIGHLIGHTS

- 19 ▪ A close comparison between the exceptional Arctic winters 2020 and 2011
- 20 ▪ Long-lasting vortex up to the end of April in 2020, but up to early April 2011
- 21 ▪ Unusually early chlorine activation and ozone loss in early January 2020
- 22 ▪ The ozone loss in 2020 is stronger in lower stratosphere than that in 2011

23

24

25

26

27

28

29

30

31

32

33

34

35

36

37 **Key words:** Climate Change; Arctic ozone; Polar Vortex; Ozone hole; Satellite measurements; Ozonesonde

38 **Short title:** Ozone loss in the Arctic winters 2011 and 2020

39

40

41

42 **ABSTRACT**

43 Polar ozone depletion has been a major environmental threat for humanity since the late 1980s. The
44 2011 Arctic winter caught much global attention because of the amount of ozone loss (2.3–3.4 ppmv at
45 450–475 K potential temperature) and a similar loss was also observed in the 2020 winter (2.5–3.5 ppmv,
46 at 400–500 K). Since the difference between the winter of 2010/11 and 2019/20 in terms of ozone loss is
47 small, we investigate the change in terms of polar processing in these winters, as that would help future
48 projections of ozone recovery in polar regions. The ozone loss estimated by different methods (passive
49 tracer and vortex descent) shows the highest loss in April in both years 2011 and 2020, but the peak
50 ozone loss altitude was different. The overall ozone loss was more extensive in the lower stratosphere in
51 2020, but relatively large loss occurred at higher altitudes in 2011. A prolonged chlorine activation was
52 evident in 2020, longer than that in 2011, which also enhanced loss in the lower stratosphere in 2020.
53 The situation in 2020 resulted in very small values of column ozone, which were below 220 DU for more
54 than three weeks, and a near-complete ozone loss (93%) at certain altitudes in the lower stratosphere.
55 The ozone loss in 2020 was similar to that in the Antarctic, and was triggered by the presence of a strong
56 and stable polar vortex with zonal winds of constant velocity (40–45 ms⁻¹) and temperature conditions
57 favoring large areas of PSCs (10 million km²) for most of the winter. The relatively lower values of
58 momentum flux suggest that the tropospheric forcing was lower in 2020. Therefore, both winters had
59 less disturbed and long-lasting polar vortices allowing lower temperatures, large areas of PSCs, and longer
60 periods of severe chlorine activation, which in turn led to record-breaking ozone loss of the levels found
61 in the Antarctic vortex, for some days.

62 1. INTRODUCTION

63 Polar stratospheric ozone loss has been a severe threat since the Antarctic ozone hole was discovered in
64 1985¹. The formation of the ozone hole resulted from emissions of ozone-depleting substances (ODSs)
65 like CFCs, bromo-halides and several other compounds originating from human activities²⁻⁶. The lower
66 temperatures and isolated air masses inside vortex in the Antarctic made the ozone hole an annually
67 recurring event, unlike in the Arctic^{7,8}. The interannual variability of the relative strength of Arctic vortex⁹
68 and the presence of higher temperature due to greater transport and mixing from the lower latitudes^{10,11}
69 significantly affect the extent of Arctic ozone depletion. For strong polar chemical ozone depletion to
70 occur, it is necessary that not only sufficiently low temperatures are reached at some point in
71 winter/spring, but also that such low temperatures, as well as high active chlorine levels, are sustained
72 into spring. The polar regions experience the strongest ozone loss in spring (late August, September, early
73 October in the Antarctic; late February, March, early April in the Arctic)¹². During these periods, high
74 active chlorine levels need to be sustained at a time when both gas-phase chlorine deactivation and
75 heterogeneous chlorine activation proceed at large rates¹³⁻¹⁶. Arctic ozone loss has been prevalent since
76 the late eighties^{17,18}. The ozone loss, however, is less pronounced than in the Antarctic because of the
77 meteorology of the Arctic winters, which is different from that of Antarctic winters^{10,19}.

78 The stratosphere in the Arctic during winter is subject to frequent tropospheric wave forcings in the
79 Northern Hemisphere (NH), and thus, culminates in Sudden Stratospheric Warming (SSW) in many
80 winters²⁰. This warming reduces ozone depletion by weakening the polar vortex²¹⁻²³. Strong Arctic ozone
81 loss is common in cold winter/spring²⁴⁻²⁶. Studies showed that the mean PSC volume (V_{psc}) and the area of
82 PSC (A_{psc}) in the Arctic in cold winters have been increasing since the late 1960s. This increase in PSC
83 volume directly implies an accelerated loss of ozone as it facilitates the activation of chlorine in the
84 presence of sunlight²⁷. This increasing depletion of ozone in the Arctic is hypothesized to climate change
85 in the stratosphere, and every one degree of cooling will result in an additional ozone loss of 15 DU^{26,28}. A

86 similar conclusion was derived in several other studies from the Arctic ozone loss observations²⁹. The
87 combination of greenhouse gas (GHG) forcing and the subsequent cooling of the stratosphere has a
88 direct impact on the stability of the Arctic polar vortex, and is found to remarkably increase the ozone
89 loss^{30–33}. The most recent study of von der Gathen et al.³⁴ concludes that if the future abundance of GHGs
90 continues to rise, it would favor a large seasonal loss of Arctic ozone. Sinnhuber et al.³⁵ report that cooling
91 of 0.8 K/decade in the Arctic winter stratosphere would counterbalance the effects of reduced
92 stratospheric halogen loading due to the Montreal Protocol. A similar offset in the predicted ozone
93 recovery due to projected stratospheric radiative cooling is also presented in the study of Bohlinger et
94 al.³⁶ The shift of polar minimum temperatures from late to early winters would induce early formation of
95 the polar vortex. Therefore, it would contribute to enhanced and prolonged ozone loss in the Arctic, as
96 mentioned in the study of Langematz et al.³⁷. The central Pacific Sea Surface Temperature (SST) warming
97 also influences the depletion of ozone in the Arctic, which contributes to the strengthening of Arctic
98 vortex in winter (DJF)³⁸. Also, the negative SST phase leads to strengthening of the vortex as found in
99 2011 due to a reduction in the planetary wave propagation^{39–41}.

100 A strong chemical ozone loss caused by a long period of low temperature in the lower stratosphere is rare
101 in the Arctic, and the earliest such ozone loss was reported for the 1995/96 winter, followed by 1996/97,
102 1999/2000, 2010/11, 2015/16, and 2019/20^{28,42–44}. Chemical ozone loss in the Arctic in 1997 was
103 supported by PSC formation and a strong polar vortex that persisted until late April^{45–47}. Similar winter
104 conditions occurred more extremely in the 2011 winter. The ozone loss was very severe such that the
105 situation that usually experiences in the Antarctic was observed^{8,11,29,35,44,48,49}. The ozone loss estimated
106 was in the order of 2.3–3.5 ppmv in late March-early April 2011, though the value differed slightly in
107 these studies due to differences in defining the vortex edge criterion, measured altitude ranges, and the
108 methods used to calculate the ozone loss. The 2015/16 winter was also distinct, but the vortex was not
109 long lasting, as it dissipated in early March 2016 due to the early final warming⁵⁰. The temperature

110 observed from December 2015 through early February 2016 was the lowest in the past 68 years, which
111 caused severe denitrification and high dehydration^{50–52}. The 2020 winter also exhibited characteristics
112 similar to the previous extreme cold winters of the Arctic (i.e., 1996/97 and 2010/11). The winter showed
113 the lowest temperature record for the past 41 years, a strong vortex that lasted until late April⁵³, ozone
114 loss rising to values similar to those observed in the 2011 winter^{54–58}, and strong denitrification. Model
115 studies of the 2020 winter also arrived at similar conclusions^{59–61}. Here, we present an in-depth analysis of
116 polar processing in both 2011 and 2020 winters and discuss the similarities and differences, as this would
117 help modeling studies and future projection of ozone recovery in the Arctic.

118 2. DATA AND METHODS

119 We use the satellite measurements of ozone, N₂O and ClO from Microwave Limb Sounder (MLS) v5^{62,63}.
120 The MLS profiles are presented in potential temperature vertical co-ordinates. It is computed using the
121 pressure and temperature data available from the MLS profiles. The MLS temperature, ozone, N₂O and
122 ClO data have an uncertainty of 2–10%, depending on the constituent, latitude and altitude region. The
123 potential vorticity (PV) values are taken from the European Centre for Medium-Range Weather Forecasts
124 (ECMWF) Reanalyses ERA5 data⁶⁴. The ozone loss calculation is performed inside the vortex, and the
125 vortex edge at different altitudes is determined using to the Nash et al.⁶⁵ criterion.
126 The vertical distribution of N₂O is exponential due to the photolysis and lack of N₂O sources in the lower
127 altitudes. The MLS N₂O data extracted from 190 GHz retrieval provides information at a pressure level of
128 68 hPa (or 400 K isentropic level). Subsequently, the data are extrapolated to 350 K by an exponential
129 fitting to the N₂O data for the 400–600 K levels. Profile descent method^{66–69} is applied for the estimation
130 of ozone loss, in which the N₂O data are used for descent calculations. The ozone loss is estimated by
131 utilizing the ozone profiles in December of the preceding year. Apart from this, ozone loss is also
132 calculated with the passive method for which a passive tracer from the SLIMCAT simulations is used^{67,70,71}.
133 The depletion is computed for each day for which the ozone measurements are subtracted from the

134 tracer each day. The meteorology of the winter is analyzed using the Modern-Era Retrospective analysis
135 for Research and Applications version 2 (MERRA-2) data⁷², and these data are available for the period
136 1980–2021.

137 3. RESULTS AND DISCUSSION

138 **3.1 Meteorology of the winters 2020 and 2011.** Figure 1 shows the monthly evolution of different
139 meteorological parameters for the years 2011 (black) and 2020 (green) along with the average for the
140 period 1980–2020 (red) in the Arctic. The top panel shows the evolution of zonal mean minimum
141 temperature for 50–90°N at 50 hPa and it is interesting to observe temperatures less than 195 K
142 (indicated by the black line) (see Grooß and Müller⁶¹; figure 10) for nearly four months in both years,
143 which is rare in the Arctic. The regions of lower temperature are significant as they are important for the
144 formation of PSCs. These clouds further help in the process of ozone loss by serving as the activation
145 surface for chlorine⁷³. The winters had a minimum temperature less than the PSC existence threshold
146 from December to March and started to rise above this value by early April, consistent with the results of
147 previous studies (e.g., Figure 1 of Manney et al.^{44,55}). Kuttippurath et al.⁴⁸ and Varotsos et al.⁷⁴ used the
148 zonal average of minimum temperatures from 40° to 90° N at 475 K and observed a similar evolution of
149 minimum temperatures below the PSC threshold for 2011. Dameris et al.⁷⁵ analyzed the mean monthly
150 minimum temperature at 50 hPa for the zonal average between 50° N and 90° N, and it showed that the
151 temperature was less than 195 K during December–March in both years. The values of temperatures
152 during the winter months are lower in 2020 (see also Alwarda et al.⁷⁶). On the other hand, the long-term
153 mean (1980–2020, red curve) shows PSC favorable temperatures only in December and January. The
154 second panel shows the development of zonal mean temperature at 60°–90° N. In 2020, the temperature
155 decreased from 210 K in early December to 204 K by mid-January. This drop, however, has been
156 compensated by a rise of the same amount towards late January 2020. The temperature shows a
157 consistent value for at least a month thereafter, but increases by mid-March. Temperature values are

158 lowest in late February 2020 and are observed to be the lowest since 1979⁵³. The winter 2020 shows
159 lower temperature values in the order of 205–208 K in the third week of February. In 2011, there were
160 two small peaks in temperature in early January and early February (see Kuttippurath et al.⁴⁸). As
161 compared to these, only one minor warming was observed in 2020, from late January to early February.

162 The third panel of Figure 1 compares the PSC area for both winters and the mean PSC area from 1980 to
163 2020 (red). The PSC area at 460 K spreads to 14 million km² in late January 2020 and stands slightly higher
164 than that in 2011 throughout the period until mid-March. The PSC area stayed around 8–10 million km²
165 for most of December, January, February, and March in both years, and was similar to that observed in
166 the Antarctic^{58,77}. The mean PSC area stayed less than 5 million km² throughout the years. An associated
167 drop in the PSC area in both winters was observed concurrent with the periods of minor warming.

168 The bottom fourth panel shows the relative strength of polar vortex in terms of zonal wind velocity (U).
169 Lawrence et al.⁵³ described the 2020 winter vortex to be the largest with an area of 20–25 million km²
170 and that lasted until late April. The zonal winds in both winters follow a constant velocity of about 30–40
171 ms⁻¹ up to late March, which is not usually observed in the Arctic winters (see Lawrence et al.⁵³). The
172 uniformity in wind speed ensures a strong polar vortex and the final warming with reversal of westerlies
173 happened around mid-April in 2011 and late April in 2020⁷⁸. The zonal wind speed at 100 and 10 hPa in
174 2020 are the highest and third highest, respectively, when compared to the winters since 1959⁵³. Thus,
175 the vortex during both winters was long lasting and stronger in 2020. A comparison of the maximum PV
176 at 475 K from 1994 to 2012 showed that the PV gradient was sharpest in 2011; indicating that the vortex
177 strength was highest in that winter²⁹.

178 The last two panels of figure 1 examine the momentum and heat fluxes during the years (2011 and 2020)
179 along with the climatology values (red). The momentum flux estimates at 60° N (100 hPa) for both years
180 show that flux is mostly negative during December, January and February (DJF), suggestive of a relatively

181 stable polar vortex. However, it is observed that the climatology values are only slightly negative ($-15 \text{ m}^2\text{s}^{-2}$).
182 2). Beyond DJF, the values become positive; indicating increased wave forcing and a less stable polar
183 vortex. The bottom panel of Figure 1 illustrates the zonally averaged 45-day mean heat flux computed
184 over the latitude region $45\text{--}75^\circ \text{ N}$ at 100 hPa. Heat fluxes in both winters are found to be below the mean
185 or climatology values until mid-April. Although the flux is directed poleward during most of the winter,
186 the range of values is small, and henceforth, the vortex was more stable in 2011 and 2020; consistent
187 with the analyses of Inness et al.⁵⁴. The model simulations performed by Rao and Garfinkel⁷⁹ also predict a
188 very stable polar vortex in the 2020 winter similar to that observed in 2011 and 1997. Lee et al.⁸⁰ reveals
189 that a possible reason for the relatively low wave forcing during the winter is due to the destructive
190 interference of tropospheric waves with the climatological stationary waves in the early winter of 2020.

191 **3.2 Evolution of the Polar Vortex.** Figure 2 shows the temporal evolution of the polar vortex in both
192 winters. The days are chosen such that the vortex begins to form in early December and becomes fully
193 formed by late January. In the following months, the vortex splits or displaces in the presence of strong
194 SSW, and remains relatively stable in the absence of SSWs. The top panel of the figure shows the initial
195 formation of the vortex in 2011. A complete and distinct vortex forms towards the end of January despite
196 the minor warming. The warming intensified in February when the vortex split into two parts. The vortex
197 recovered soon after the temperature lowered and thus, reformed a pole-centered circular vortex
198 thereafter in early March. It remained intact until early April, which was in agreement with the previous
199 studies⁴⁸. In 2020, a large vortex was formed in early January as illustrated in the PV maps. The areal
200 spread of vortex was larger in 2020 than that in the 2011 winter. The prolonged appearance of low
201 temperatures, which is quite unusual compared to the observations in the past 41 years (1979/80 -
202 2019/20), led to a strong and stable vortex in 2020⁵⁶. Despite the minor warming in late January, the
203 vortex remained strong until late April. Eventually, at the end of April, the vortex splits into two lobes. The
204 location of vortex in either of these winters was pole-centered although its spatial spread extended up to

205 the mid-latitudes⁷⁵. A detailed comparison of relevant meteorological parameters for both winters is
206 presented in Table 1.

207 Important parameters that possibly affect the strength of polar vortex are the external influences, such as
208 Quasi-Biennial Oscillation (QBO), El Nino Southern Oscillations (ENSO), Eurasian snow cover, solar cycle,
209 and several others^{81–83}. The strength of the vortex is higher in the westerly phase of QBO (in the tropical
210 lower stratosphere at ~50 hPa) by the Holton-Tan relationship⁸⁴. The QBO was westerly during the 2011
211 winter⁸⁵. The QBO and ENSO were both nearly neutral in the 2020 winter⁷⁹. The 2011 winter witnessed
212 the La Nina phase⁸⁶. Thus, these external influences also impacted positively on the vortex by reducing
213 the severity of tropospheric forcing and thus, strengthening the vortex.

214 **3.3 Diabatic Descent and Chlorine Activation in 2020 and 2011.** Figure 3 shows the distribution of O₃, ClO,
215 N₂O, and HNO₃, derived for the winters using satellite observations. Data corresponding to the temporal
216 evolution of trace gases are obtained from MLS on the Aura satellite. There is a substantial increase in
217 the concentration of N₂O in the lower stratosphere, indicating the dynamic descent in the stratosphere.
218 The descent rate is greater in 2020 than in 2011 when the N₂O isolines are followed (third panel of Figure
219 3, also see Feng et al.⁶⁰). The N₂O values decrease rapidly to as low as 50 ppbv from 250–300 ppbv at 400
220 K altitude from December to April in 2020, but the range of values stays around 150–250 ppbv at 400 K in
221 2011. Similar diabatic descent rates in 2020 are also reported by Grooß and Müller⁶¹ using CLaMS
222 simulations and ACE-FTS measurements. However, that study was carried out for the days between 23
223 and 29 March, and the simulations showed slower descent, though the range is similar to that in our
224 analysis. Manney et al.⁵⁵ observed a lower than normal concentration of N₂O in the lower stratosphere in
225 2020, which was caused by the increased descent from the mid-stratosphere.

226 In general, chlorine activation in the Arctic begins in early January and continues until late February⁴³. The
227 period of activation implies a strong association between PSC existence and the temperatures of chlorine

228 activation. The highest chlorine activation is observed during the coldest periods of the winters; i.e.,
229 January and February. In 2011, the ClO concentrations reached 1.6 ppbv in January and the chlorine
230 activation was present up to late March when the ClO values dropped to less than 1 ppbv (500–600 K).
231 Conversely, the ClO concentration was higher than 1.7 ppbv in late December 2020 at 500–600K⁵⁵. Unlike
232 the usual winters, the enhanced concentration of ClO in 2020 was not only restricted to the altitudes at
233 500–550 K, but also was present between 500 and 600 K for almost a month. The chlorine levels declined
234 soon after January 2020 and were negligible in early February 2020. A possible reason that decelerated
235 the chlorine activation is the minor warming in early February 2020. However, the chlorine activation in
236 2011 continued even after January and persisted until late March (500–550 K). Therefore, similar to the
237 results of Manney et al.⁵⁵ chlorine activation in the higher altitudes was stronger in 2011 than in 2020
238 (see also Inness et al.⁵⁴). The ozone loss during the winters is comparable because of the compensating
239 spatial distribution of ClO in both winters. The record-high chlorine activation observed in 2011 is also
240 discussed in Adams et al.⁸⁷ and Kuttippurath et al.⁴⁸.

241 The 2020 winter shows a proportional relationship between the period of lowest temperature and severe
242 denitrification. The concentration of HNO₃ is important to analyze the denitrification in the period. The
243 concentration of HNO₃ in the lower stratosphere was above 12 ppbv in early December 2011, compared
244 to 9 ppbv in 2020. The seasonal evolution from winter to spring further reduces the concentration of
245 HNO₃ due to photolysis⁸⁸. The concentration of HNO₃ in early spring is lower by about 60–80% than in
246 early winter 2020⁵⁷, opposed to the 40–50% denitrification in 2011^{35,48}. The minor warming in late
247 January subsides the rate of denitrification for that particular period in 2020. The bottom panel of figure 3
248 shows the temporal evolution of ozone concentration. The maximum concentration of ozone is limited to
249 the middle (550–700 K) and upper stratosphere (850 K and above) whereas the lowest ozone
250 concentration occupies the 350–500 K altitude region (lower stratosphere). The denitrification was severe
251 in both winters of 2011 and 2020. A similar rate of high vortex-wide denitrification had also been

252 reported in the Arctic winter 2016^{29,44,89}. The highest ozone concentration in Figure 4 is observed in the
253 upper stratosphere in both years and is the highest in April for 2020 (5–6 ppmv) and March for 2011 (4–5
254 ppmv) (note that the MLS data are not available in April 2011). The smallest concentration of ozone is
255 observed in the lower stratosphere and is lower than 1 ppmv. The period of lowest concentration is found
256 to be coherent with the period of peak chlorine activation and denitrification.

257 The increased rate of vortex descent, accelerated denitrification and enhanced chlorine activation in
258 2020, make it more conducive for the large ozone loss. The ozone concentrations began to decline earlier
259 in 2020 and the loss was also slightly higher than that in 2011 in the lower stratosphere, below 550 K. The
260 loss was observed at 400–650 K in December and the loss became more apparent in the lower
261 stratosphere thereafter in the minor warming period. The amount of ozone in the lower stratosphere is
262 between 1 and 3 ppmv in both winters in December, but it reduced to less than 1.5 ppmv in March and
263 April, as depicted in the figures. The difference between both winters is mostly about the onset of loss
264 and the peak ozone loss period. The unusual ozone loss since December is very particular to 2020 and the
265 loss is slightly higher in 2020 than that in 2011. The measurements show exceptionally smaller values of
266 ozone, about 0.5 ppmv or below, from mid-March to the end of April at 350–450 K in 2020. Due to the
267 unavailability of MLS data in April 2011, a gap is shown in the analyses for that period, which also makes
268 the comparison between the winters for the period slightly difficult. The lowermost panel of Figure 4
269 shows the difference in the concentration of ozone in both winters and is mostly smaller than 1 ppmv.

270 **3.4 Ozone loss in the winters 2020 and 2011.** A method suitable to calculate the chemical ozone loss
271 neglecting the impact of the mixing process and other dynamic processes is the vortex descent
272 method^{69,90}. We have analysed the chemical ozone loss by applying the vortex descent method. In
273 addition, the passive tracer method is also used to calculate ozone loss. The ozone loss is computed by
274 finding the difference of passive ozone simulated from SLIMCAT from measured ozone⁹¹. Figure 4 shows

275 the chemical ozone loss estimated using the MLS measurements for the winters 2020 and 2011. The
276 ozone loss as mentioned previously is estimated by the vortex descent and by the passive method using
277 the simulations from the chemical transport model (CTM), SLIMCAT⁹². As the ozone loss is evaluated with
278 respect to the MLS data, there is a corresponding gap in 2011 due to the lack of measurements in early
279 April 2011.

280 The ozone loss reached a maximum of 2.4 ppmv at 350–475K in March 2011. The loss in the lower
281 stratosphere shows more than 2.5 ppmv in March 2020. In the middle stratosphere above 450 K, the
282 ozone loss is larger in 2011 than that in 2020. However, the ozone loss in the upper stratosphere shows a
283 similar value in both winters. The difference in the ozone loss between the winters is that it stays around
284 +(0.2–0.5) ppmv in 2020 compared to less than -(0.6–0.7) ppmv in 2011 in the middle stratosphere. The
285 ozone loss estimated by the passive method for the winter 2011 by Manney et al.⁴⁴, Kuttippurath et al.⁴⁸,
286 Sinnhuber et al.³⁵, and Griffin et al.⁶⁹ shows about 2.1–2.5 ppmv at 450–550 K. The ozone loss estimated
287 by Wohltmann et al.⁵⁶ shows 2.2 ppmv at 450K in 2020 and 2.5 ppm at 490 K in 2011. They find that the
288 ozone loss amount in the 2011 winter was higher probably because of the greater transport of ozone
289 from lower altitudes in that winter, though the percentage of ozone loss was higher in 2020 (73%) than
290 that in 2011 (63%). The 2011 ozone loss determined by the Match method in the study of Livesey et al.⁹³
291 presented a loss of 2.0 ppmv at 450 K. Manney et al.⁵⁵ estimated the ozone loss for both winters using
292 the Match method and found a loss of about 2.8 ppmv in the lower stratosphere. They also showed that
293 the loss in lower altitudes in 2020 was larger than that in 2011; consistent with the results from the
294 studies by Kuttippurath et al.⁵⁷, Inness et al.⁵⁴, Grooß and Müller⁶¹, and Dameris et al.⁷⁵, although there is
295 a slight difference in the loss calculated in percent. Figure 6 summarizes and further compares the ozone
296 losses in various studies for both winters.

297 The vertical profiles show an early onset of the ozone loss in the upper stratosphere in December of the
298 order of 0.5–0.6 ppbv in 2020, but close to zero in 2011 (Figure 5). In the lower stratosphere, the ozone
299 loss situation in both years is similar in December with little loss. The ozone loss occurred in January and
300 February is higher in 2020, and the loss reached up to 1.5 ppbv in January and 2.5 ppbv in February 2020.
301 In 2011, the loss was less than 0.5 ppbv, and the pattern of loss is the same in the upper stratosphere in
302 both years, even though the standard deviation is higher in 2020. The highest ozone loss was measured in
303 the lower stratosphere in April followed by March in 2020^{54,57}. The loss in April 2020 was about 2.5 ppbv
304 though the standard deviation reaches up to 3.5 ppbv. However, the loss is very small and is close to zero
305 in the upper stratosphere. The interesting aspect here is that there is higher ozone loss compared to the
306 previous winters in the upper stratosphere, about 0.5 ppbv in March and April in both winters; which
307 suggests the relatively higher ozone loss in these years.

308 To examine the extreme ozone loss in these winters, we considered the total column ozone (TCO, Figure
309 6). The ozone maps clearly show that the values never dropped below 220 DU on any day in 2011, but
310 there were more than three weeks in which TCO dropped below that threshold in 2020. The severity of
311 this winter and extreme ozone loss is further investigated using ozonesonde measurements (bottom,
312 Figure 6). The ozonesonde measurements at Alert and Eureka show near-complete loss of ozone or loss
313 saturation in 2020 in some days (80–93% loss). Conversely, the ozonesonde measurements in 2011 never
314 experienced the loss saturation or such low ozone values as observed in 2020 at any altitude. Therefore,
315 both total column and ozonesonde measurements attest that the winter 2020 was unprecedented and
316 was colder, denitrified, chlorine activated and ozone depleted than those in 2011.

317 4. CONCLUSION

318 The very strong Arctic ozone loss in the 2020 winter has turned out to be a matter of severe interest for
319 the human community globally⁹⁴. Bernhard et al.⁹⁵ observed a 140% increase in the measurements of the

320 ultraviolet index (UVI) for several days in 2020 compared to previous years. The severe ozone loss in the
321 Arctic would affect a major part of the population in the surrounding land regions^{34,96}. There are studies
322 that show that stratospheric ozone is recovering globally, but not in the Arctic, yet^{12,62}. The reason is the
323 reduction of atmospheric chlorine levels caused by the Montreal Protocol and its amendments and
324 adjustments. Arctic ozone would have developed into an Antarctic-like ozone hole if not for the Montreal
325 Protocol⁹⁷. The 2020 winter showed severe ozone loss in the order of 2.5 ppmv in the altitude range
326 between 400 and 500 K. The magnitude of the loss in 2011 was slightly lower and remained to same
327 altitude range, particularly below 475 K. The conditions that made 2020 winter conducive to ozone loss
328 were the long-lasting low temperatures in the lower stratosphere, where the minimum temperature
329 remained below the PSC existence threshold for more than a month, giving rise to large areas of PSCs and
330 a prolonged severe chlorine activation. The early start of the ozone loss in 2020 as compared to that in
331 2011 is identified by the beginning of PSC formation. The vortex in both winters remained undisturbed
332 until early April and late April in 2011 and 2020, respectively. Thus, our study indicates that winter 2020
333 had a very low temperature, long-lasting and undisturbed vortex, slightly higher chlorine activation and
334 larger ozone loss than that in 2011. In 2020, the Arctic winter also experienced a near-complete loss of
335 ozone and TCO values lower than 220 DU for more than 23 days. The comparison of the Arctic winters of
336 2011 and 2020, as presented here, therefore, could contribute to modeling studies of the processes of
337 ozone loss chemistry and projection of ozone recovery.

338 REFERENCES

- 339 (1) Farman, J. C.; Gardiner, B. G.; Shanklin, J. D. Large Losses of Total Ozone in Antarctica Reveal
340 Seasonal ClO_x/NO_x Interaction. *Nature* **1985**, *315*, 207–210. DOI: 10.1038/315207a0.
- 341 (2) Molina, M. J.; Rowland, F. S. Stratospheric Sink for Chlorofluoromethanes: Chlorine Atom-
342 Catalysed Destruction of Ozone. *Nature* **1974**, *249*, 810–812. DOI: 10.1038/249810a0.
- 343 (3) Stolarski, R. S.; Cicerone, R. J. Stratospheric Chlorine: A Possible Sink for Ozone. *Can. J. Chem.*
344 **1974**, *52*, 1615. DOI: 10.1139/v74-233.

345 (4) Wofsy, S. C.; McElroy, M. B.; Yung, Y. L. The Chemistry of Atmospheric Bromine. *Geophys. Res. Lett.* **1975**, *2*, 215–218. DOI: 10.1029/GL002I006P00215.

346

347 (5) McElroy, M. B.; Salawitch, R. J.; Wofsy, S. C.; Logan, J. A. Reductions of Antarctic Ozone Due to Synergistic Interactions of Chlorine and Bromine. *Nature* **1986**, *321*, 759–762. DOI: 10.1038/321759a0.

348

349 (6) Rowland, S. F. Stratospheric Ozone Depletion by Chlorofluorocarbons. *Ambio* **1990**, *19*, 281–292.

350 (7) Solomon, S.; Portmann, R. W.; Thompson, D. W. J. Contrasts between Antarctic and Arctic Ozone Depletion. *Proc. Natl. Acad. Sci.* **2007**, *104*, 445–449. DOI: 10.1073/PNAS.0604895104.

351 (8) Solomon, S.; Haskins, J.; Ivy, D. J.; Min, F. Fundamental Differences between Arctic and Antarctic Ozone Depletion. *Proc. Natl. Acad. Sci.* **2014**, *111*, 6220–6225. DOI: 10.1073/PNAS.1319307111.

352 (9) Schoeberl, M. R.; Hartmann, D. L. The Dynamics of the Stratospheric Polar Vortex and Its Relation to Springtime Ozone Depletions. *Science*. **1991**, *251*, 46–52. DOI: 10.1126/SCIENCE.251.4989.46.

353 (10) Tegtmeier, S.; Rex, M.; Wohltmann, I.; Krüger, K. Relative Importance of Dynamical and Chemical Contributions to Arctic Wintertime Ozone. *Geophys. Res. Lett.* **2008**, *35*, L17801. DOI: 10.1029/2008GL034250.

354 (11) Strahan, S. E.; Douglass, A. R.; Newman, P. A. The Contributions of Chemistry and Transport to Low Arctic Ozone in March 2011 Derived from Aura MLS Observations. *J. Geophys. Res. Atmos.* **2013**, *118*, 1563–1576. DOI: 10.1002/JGRD.50181.

355 (12) WMO (World Meteorological Organization), *Scientific Assessment of Ozone Depletion: 2018*, Global Ozone Research and Monitoring Project – Report No. 58, 588 Pp., Geneva. 2018. (accessed 09/28/2021).

356 (13) Portmann, R. W.; Solomon, S.; Garcia, R. R.; Thomason, L. W.; Poole, L. R.; McCormick, M. P. Role of Aerosol Variations in Anthropogenic Ozone Depletion in the Polar Regions. *J. Geophys. Res. Atmos.* **1996**, *101*, 22991–23006. DOI: 10.1029/96JD02608.

357 (14) Grooß, J. U.; Brauttsch, K.; Pommrich, R.; Solomon, S.; Müller, R. Stratospheric Ozone Chemistry in the Antarctic: What Determines the Lowest Ozone Values Reached and Their Recovery? *Atmos. Chem. Phys.* **2011**, *11*, 12217–12226. DOI: 10.5194/ACP-11-12217-2011.

358 (15) Solomon, S.; Kinnison, D.; Bandoro, J.; Garcia, R. Simulation of Polar Ozone Depletion: An Update. *J. Geophys. Res. Atmos.* **2015**, *120*, 7958–7974. DOI: 10.1002/2015JD023365.

359 (16) Müller, R.; Grooß, J. U.; Mannan Zafar, A.; Robrecht, S.; Lehmann, R. The Maintenance of Elevated Active Chlorine Levels in the Antarctic Lower Stratosphere through HCl Null Cycles. *Atmos. Chem. Phys.* **2018**, *18*, 2985–2997. DOI: 10.5194/ACP-18-2985-2018.

360

361

362

363

364

365

366

367

368

369

370

371

372

373

374

375

376

- 377 (17) Solomon, S. Stratospheric Ozone Depletion: A Review of Concepts and History. *Rev. Geophys.*
378 **1999**, *37*, 275–316. DOI: 10.1029/1999RG900008.
- 379 (18) Müller, R.; Grooß, J. U.; Lemmen, C.; Heinze, D.; Dameris, M.; Bodeker, G. Simple Measures of
380 Ozone Depletion in the Polar Stratosphere. *Atmos. Chem. Phys.* **2008**, *8*, 251–264. DOI:
381 10.5194/ACP-8-251-2008.
- 382 (19) Chipperfield, M. P.; Jones, R. L. Relative Influences of Atmospheric Chemistry and Transport on
383 Arctic Ozone Trends. *Nat. 1999 4006744* **1999**, *400*, 551–554. DOI: 10.1038/22999.
- 384 (20) Butler, A. H.; Gerber, E. P. Optimizing the Definition of a Sudden Stratospheric Warming. *J. Clim.*
385 **2018**, *31*, 2337–2344. DOI: 10.1175/JCLI-D-17-0648.1.
- 386 (21) Kuttippurath, J.; Nikulin, G. Atmospheric Chemistry and Physics. *Atmos. Chem. Phys* **2012**, *12*,
387 8115–8129. DOI: 10.5194/acp-12-8115-2012.
- 388 (22) Manney, G. L.; Lawrence, Z. D.; Santee, M. L.; Read, W. G.; Livesey, N. J.; Lambert, A.; Froidevaux,
389 L.; Pumphrey, H. C.; Schwartz, M. J. A Minor Sudden Stratospheric Warming with a Major Impact:
390 Transport and Polar Processing in the 2014/2015 Arctic Winter. *Geophys. Res. Lett.* **2015**, *42*,
391 7808–7816. DOI: 10.1002/2015GL065864.
- 392 (23) De La Cámara, A.; Abalos, M.; Hitchcock, P.; Calvo, N.; Garcia, R. R. Response of Arctic Ozone to
393 Sudden Stratospheric Warmings. *Atmos. Chem. Phys.* **2018**, *18*, 16499–16513. DOI: 10.5194/acp-
394 18-16499-2018.
- 395 (24) Müller, R.; Crutzen, P. J.; Grooß, J.-U.; Bürl, C.; Russell, J. M.; Gernandt, H.; McKenna, D. S.; Tuck,
396 A. F. Severe Chemical Ozone Loss in the Arctic during the Winter of 1995–96. *Nature* **1997**, *389*,
397 709–712. DOI: 10.1038/39564.
- 398 (25) Pawson, S.; Naujokat, B. The Cold Winters of the Middle 1990s in the Northern Lower
399 Stratosphere. *J. Geophys. Res. Atmos.* **1999**, *104*, 14209–14222. DOI: 10.1029/1999JD900211.
- 400 (26) Rex, M.; Salawitch, R. J.; von der Gathen, P.; Harris, N. R. P.; Chipperfield, M. P.; Naujokat, B. Arctic
401 Ozone Loss and Climate Change. *Geophys. Res. Lett.* **2004**, *31*, L04116. DOI:
402 10.1029/2003GL018844.
- 403 (27) Harris, N. R. P.; Lehmann, R.; Rex, M.; Von Der Gathen, P. A Closer Look at Arctic Ozone Loss and
404 Polar Stratospheric Clouds. *Atmos. Chem. Phys.* **2010**, *10*, 8499–8510. DOI: 10.5194/ACP-10-8499-
405 2010.
- 406 (28) Rex, M.; Salawitch, R. J.; Deckelmann, H.; von der Gathen, P.; Harris, N. R. P.; Chipperfield, M. P.;
407 Naujokat, B.; Reimer, E.; Allaart, M.; Andersen, S. B.; Bevilacqua, R.; Braathen, G. O.; Claude, H.;
408 Davies, J.; De Backer, H.; Dier, H.; Dorokhov, V.; Fast, H.; Gerding, M.; Godin-Beekmann, S.;

- 409 Hoppel, K.; Johnson, B.; Kyrö, E.; Litynska, Z.; Moore, D.; Nakane, H.; Parrondo, M. C.; Risley, A. D.;
410 Skrivankova, P.; Stübi, R.; Viatte, P.; Yushkov, V.; Zerefos, C. Arctic Winter 2005: Implications for
411 Stratospheric Ozone Loss and Climate Change. *Geophys. Res. Lett.* **2006**, *33*, L23808. DOI:
412 10.1029/2006GL026731.
- 413 (29) Pommereau, J. P.; Goutail, F.; Lefèvre, F.; Pazmino, A.; Adams, C.; Dorokhov, V.; Eriksen, P.; Kivi, R.;
414 Stebel, K.; Zhao, X.; Van Roozendaal, M. Why Unprecedented Ozone Loss in the Arctic in 2011? Is
415 It Related to Climate Change? *Atmos. Chem. Phys.* **2013**, *13*, 5299–5308. DOI: 10.5194/ACP-13-
416 5299-2013.
- 417 (30) Shindell, D. T.; Rind, D.; Loneragan, P. Increased Polar Stratospheric Ozone Losses and Delayed
418 Eventual Recovery Owing to Increasing Greenhouse-Gas Concentrations. *Nature* **1998**, *392*, 589–
419 592. DOI: 10.1038/33385.
- 420 (31) Langematz, U. An Estimate of the Impact of Observed Ozone Losses on Stratospheric
421 Temperature. *Geophys. Res. Lett.* **2000**, *27*, 2077–2080. DOI: 10.1029/2000GL011440.
- 422 (32) WMO (World Meteorological Organization), *Scientific Assessment of Ozone Depletion: 2002*,
423 Global Ozone Research and Monitoring Project - Report No. 47, 498pp; Geneva, 2003. (accessed
424 09/28/2021).
- 425 (33) Stolarski, R. S.; Douglass, A. R.; Newman, P. A.; Pawson, S.; Schoeberl, M. R. Relative Contribution
426 of Greenhouse Gases and Ozone-Depleting Substances to Temperature Trends in the
427 Stratosphere: A Chemistry–Climate Model Study. *J. Clim.* **2010**, *23*, 28–42. DOI:
428 10.1175/2009JCLI2955.1.
- 429 (34) von der Gathen, P.; Kivi, R.; Wohltmann, I.; Salawitch, R. J.; Rex, M. Climate Change Favours Large
430 Seasonal Loss of Arctic Ozone. *Nat. Commun.* **2021**, *12*, 1–17. DOI: 10.1038/s41467-021-24089-6.
- 431 (35) Sinnhuber, B. M.; Stiller, G.; Ruhnke, R.; Von Clarmann, T.; Kellmann, S.; Aschmann, J. Arctic Winter
432 2010/2011 at the Brink of an Ozone Hole. *Geophys. Res. Lett.* **2011**, *38*, L24814. DOI:
433 10.1029/2011GL049784.
- 434 (36) Bohlinger, P.; Sinnhuber, B. M.; Ruhnke, R.; Kirner, O. Radiative and Dynamical Contributions to
435 Past and Future Arctic Stratospheric Temperature Trends. *Atmos. Chem. Phys.* **2014**, *14*, 1679–
436 1688. DOI: 10.5194/ACP-14-1679-2014.
- 437 (37) Langematz, U.; Meul, S.; Grunow, K.; Romanowsky, E.; Oberländer, S.; Abalichin, J.; Kubin, A.
438 Future Arctic Temperature and Ozone: The Role of Stratospheric Composition Changes. *J.*
439 *Geophys. Res. Atmos.* **2014**, *119*, 2092–2112. DOI: 10.1002/2013JD021100.
- 440 (38) Hu, D.; Guan, Z.; Tian, W.; Ren, R. Recent Strengthening of the Stratospheric Arctic Vortex

- 441 Response to Warming in the Central North Pacific. *Nat. Commun.* **2018**, *9*, 1697. DOI:
442 10.1038/s41467-018-04138-3.
- 443 (39) Hurwitz, M. M.; Newman, P. A.; Garfinkel, C. I. On the Influence of North Pacific Sea Surface
444 Temperature on the Arctic Winter Climate. *J. Geophys. Res.* **2012**, *117*, D19110. DOI:
445 10.1029/2012JD017819.
- 446 (40) Woo, S.-H.; Sung, M.-K.; Son, S.-W.; Kug, J.-S. Connection between Weak Stratospheric Vortex
447 Events and the Pacific Decadal Oscillation. *Clim. Dyn.* **2015**, *45*, 3481–3492. DOI: 10.1007/S00382-
448 015-2551-Z.
- 449 (41) Liu, M.; Hu, D.; Zhang, F. Connections Between Stratospheric Ozone Concentrations Over the
450 Arctic and Sea Surface Temperatures in the North Pacific. *J. Geophys. Res. Atmos.* **2020**, *125*,
451 e2019JD031690. DOI: 10.1029/2019JD031690.
- 452 (42) Popp, P. J.; Northway, M. J.; Holecek, J. C.; Gao, R. S.; Fahey, D. W.; Elkins, J. W.; Hurst, D. F.;
453 Romashkin, P. A.; Toon, G. C.; Sen, B.; Schauffler, S. M.; Salawitch, R. J.; Webster, C. R.; Herman, R.
454 L.; Jost, H.; Bui, T. P.; Newman, P. A.; Lait, L. R. Severe and Extensive Denitrification in the 1999–
455 2000 Arctic Winter Stratosphere. *Geophys. Res. Lett.* **2001**, *28*, 2875–2878. DOI:
456 10.1029/2001GL013132.
- 457 (43) Tilmes, S.; Müller, R.; Grooß, J. U.; Russell, J. M. Ozone Loss and Chlorine Activation in the Arctic
458 Winters 1991-2003 Derived with the Tracer-Tracer Correlations. *Atmos. Chem. Phys.* **2004**, *4*,
459 2181–2213. DOI: 10.5194/ACP-4-2181-2004.
- 460 (44) Manney, G. L.; Santee, M. L.; Rex, M.; Livesey, N. J.; Pitts, M. C.; Veefkind, P.; Nash, E. R.;
461 Wohltmann, I.; Lehmann, R.; Froidevaux, L.; Poole, L. R.; Schoeberl, M. R.; Haffner, D. P.; Davies, J.;
462 Dorokhov, V.; Gernandt, H.; Johnson, B.; Kivi, R.; Kyrö, E.; Larsen, N.; Levelt, P. F.; Makshtas, A.;
463 McElroy, C. T.; Nakajima, H.; Parrondo, M. C.; Tarasick, D. W.; von der Gathen, P.; Walker, K. A.;
464 Zinoviev, N. S. Unprecedented Arctic Ozone Loss in 2011. *Nat. 2011* **2011**, *478*, 469–475. DOI:
465 10.1038/nature10556.
- 466 (45) Coy, L.; Nash, E. R.; Newman, P. A. Meteorology of the Polar Vortex: Spring 1997. *Geophys. Res.*
467 *Lett.* **1997**, *24*, 2693–2696. DOI: 10.1029/97GL52832.
- 468 (46) Manney, G. L.; Froidevaux, L.; Santee, M. L.; Zurek, R. W.; Waters, J. W. MLS Observations of Arctic
469 Ozone Loss in 1996–97. *Geophys. Res. Lett.* **1997**, *24*, 2697–2700. DOI: 10.1029/97GL52827.
- 470 (47) Santee, M. L.; Manney, G. L.; Froidevaux, L.; Zurek, R. W.; Waters, J. W. MLS Observations of ClO
471 and HNO₃ in the 1996–97 Arctic Polar Vortex. *Geophys. Res. Lett.* **1997**, *24*, 2713–2716. DOI:
472 10.1029/97GL52830.

- 473 (48) Kuttippurath, J.; Godin-Beekmann, S.; Lefevre, F.; Nikulin, G.; Santee, M. L.; Froidevaux, L. Record-
474 Breaking Ozone Loss in the Arctic Winter 2010/2011: Comparison with 1996/1997. *Atmos. Chem.*
475 *Phys.* **2012**, *12*, 7073–7085. DOI: 10.5194/ACP-12-7073-2012.
- 476 (49) Hommel, R.; Eichmann, K. U.; Aschmann, J.; Bramstedt, K.; Weber, M.; Von Savigny, C.; Richter, A.;
477 Rozanov, A.; Wittrock, F.; Khosrawi, F.; Bauer, R.; Burrows, J. P. Chemical Ozone Loss and Ozone
478 Mini-Hole Event during the Arctic Winter 2010/2011 as Observed by SCIAMACHY and GOME-2.
479 *Atmos. Chem. Phys.* **2014**, *14*, 3247–3276. DOI: 10.5194/ACP-14-3247-2014.
- 480 (50) Manney, G. L.; Lawrence, Z. D. The Major Stratospheric Final Warming in 2016: Dispersal of Vortex
481 Air and Termination of Arctic Chemical Ozone Loss. *Atmos. Chem. Phys.* **2016**, *16*, 15371–15396.
482 DOI: 10.5194/ACP-16-15371-2016.
- 483 (51) Matthias, V.; Dörnbrack, A.; Stober, G. The Extraordinarily Strong and Cold Polar Vortex in the
484 Early Northern Winter 2015/2016. *Geophys. Res. Lett.* **2016**, *43*, 12287–12294. DOI:
485 10.1002/2016GL071676.
- 486 (52) Khosrawi, F.; Kirner, O.; Sinnhuber, B. M.; Johansson, S.; Höpfner, M.; Santee, M. L.; Froidevaux, L.;
487 Ungermann, J.; Ruhnke, R.; Woiwode, W.; Oelhaf, H.; Braesicke, P. Denitrification, Dehydration
488 and Ozone Loss during the 2015/2016 Arctic Winter. *Atmos. Chem. Phys.* **2017**, *17*, 12893–12910.
489 DOI: 10.5194/ACP-17-12893-2017.
- 490 (53) Lawrence, Z. D.; Perlwitz, J.; Butler, A. H.; Manney, G. L.; Newman, P. A.; Lee, S. H.; Nash, E. R. The
491 Remarkably Strong Arctic Stratospheric Polar Vortex of Winter 2020: Links to Record-Breaking
492 Arctic Oscillation and Ozone Loss. *J. Geophys. Res. Atmos.* **2020**, *125*, e2020JD033271. DOI:
493 10.1029/2020JD033271.
- 494 (54) Inness, A.; Chabrillat, S.; Flemming, J.; Huijnen, V.; Langenrock, B.; Nicolas, J.; Polichtchouk, I.;
495 Razinger, M. Exceptionally Low Arctic Stratospheric Ozone in Spring 2020 as Seen in the CAMS
496 Reanalysis. *J. Geophys. Res. Atmos.* **2020**, *125*, e2020JD033563. DOI: 10.1029/2020JD033563.
- 497 (55) Manney, G. L.; Livesey, N. J.; Santee, M. L.; Froidevaux, L.; Lambert, A.; Lawrence, Z. D.; Millán, L.
498 F.; Neu, J. L.; Read, W. G.; Schwartz, M. J.; Fuller, R. A. Record-Low Arctic Stratospheric Ozone in
499 2020: MLS Observations of Chemical Processes and Comparisons With Previous Extreme Winters.
500 *Geophys. Res. Lett.* **2020**, *47*, e2020GL089063. DOI: 10.1029/2020GL089063.
- 501 (56) Wohltmann, I.; von der Gathen, P.; Lehmann, R.; Maturilli, M.; Deckelmann, H.; Manney, G. L.;
502 Davies, J.; Tarasick, D.; Jepsen, N.; Kivi, R.; Lyall, N.; Rex, M. Near-Complete Local Reduction of
503 Arctic Stratospheric Ozone by Severe Chemical Loss in Spring 2020. *Geophys. Res. Lett.* **2020**, *47*,
504 e2020GL089547. DOI: 10.1029/2020GL089547.

505
506
507
508
509
510
511
512
513
514
515
516
517
518
519
520
521
522
523
524
525
526
527
528
529
530
531
532
533
534
535
536

- (57) Kuttippurath, J.; Feng, W.; Müller, R.; Kumar, P.; Raj, S.; Gopikrishnan, G. P.; Roy, R. Exceptional Loss in Ozone in the Arctic Winter/Spring of 2019/2020. *Atmos. Chem. Phys.* **2021**, *21*, 14019–14037. DOI: 10.5194/ACP-21-14019-2021.
- (58) Weber, M.; Arosio, C.; Feng, W.; Dhomse, S. S.; Chipperfield, M. P.; Meier, A.; Burrows, J. P.; Eichmann, K. U.; Richter, A.; Rozanov, A. The Unusual Stratospheric Arctic Winter 2019/20: Chemical Ozone Loss From Satellite Observations and TOMCAT Chemical Transport Model. *J. Geophys. Res. Atmos.* **2021**, *126*, e2020JD034386. DOI: 10.1029/2020JD034386.
- (59) Rao, J.; Garfinkel, C. I.; White, I. P. Predicting the Downward and Surface Influence of the February 2018 and January 2019 Sudden Stratospheric Warming Events in Subseasonal to Seasonal (S2S) Models. *J. Geophys. Res. Atmos.* **2020**, *125*, e2019JD031919. DOI: 10.1029/2019JD031919.
- (60) Feng, W.; Dhomse, S. S.; Arosio, C.; Weber, M.; Burrows, J. P.; Santee, M. L.; Chipperfield, M. P. Arctic Ozone Depletion in 2019/20: Roles of Chemistry, Dynamics and the Montreal Protocol. *Geophys. Res. Lett.* **2021**, *48*, e2020GL091911. DOI: 10.1029/2020GL091911.
- (61) Grooß, J.-U.; Müller, R. Simulation of Record Arctic Stratospheric Ozone Depletion in 2020. *J. Geophys. Res. Atmos.* **2021**, *126*, e2020JD033339. DOI: 10.1029/2020JD033339.
- (62) Kuttippurath, J.; Kumar, P.; Nair, P. J.; Pandey, P. C. Emergence of Ozone Recovery Evidenced by Reduction in the Occurrence of Antarctic Ozone Loss Saturation. *npj Clim. Atmos. Sci.* **2018**, *1*, 42. DOI: 10.1038/s41612-018-0052-6.
- (63) Livesey, N. J. .; Read, W. G.; Wagner, P. A.; Froidevaux, L.; Lambert, A.; Manney, G. L.; Valle, L. F. M.; Pumphrey, H. C.; Santee, M. L.; Schwartz, M. J.; Wang, S.; Fuller, R. A.; Jarnot, R. F.; Knosp, B. W.; Martinez, E.; Lay, R. R. *Version 4.2x Level 2 and 3 data quality and description document, JPL D-33509 Rev. E*. Jet Propulsion Laboratory, California Institute of Technology, Pasadena, California, 2020. https://mls.jpl.nasa.gov/data/v4-2_data_quality_document.pdf (accessed 09/28/2021).
- (64) Hersbach, H.; Bell, B.; Berrisford, P.; Hirahara, S.; Horányi, A.; Muñoz-Sabater, J.; Nicolas, J.; Peubey, C.; Radu, R.; Schepers, D.; Simmons, A.; Soci, C.; Abdalla, S.; Abellan, X.; Balsamo, G.; Bechtold, P.; Biavati, G.; Bidlot, J.; Bonavita, M.; Chiara, G. De; Dahlgren, P.; Dee, D.; Diamantakis, M.; Dragani, R.; Flemming, J.; Forbes, R.; Fuentes, M.; Geer, A.; Haimberger, L.; Healy, S.; Hogan, R. J.; Hólm, E.; Janisková, M.; Keeley, S.; Laloyaux, P.; Lopez, P.; Lupu, C.; Radnoti, G.; Rosnay, P. de; Rozum, I.; Vamborg, F.; Villaume, S.; Thépaut, J.-N. The ERA5 Global Reanalysis. *Q. J. R. Meteorol. Soc.* **2020**, *146*, 1999–2049. DOI: 10.1002/QJ.3803.
- (65) Nash, E. R.; Newman, P. A.; Rosenfield, J. E.; Schoeberl, M. R. An Objective Determination of the Polar Vortex Using Ertel’s Potential Vorticity. *J. Geophys. Res. Atmos.* **1996**, *101*, 9471–9478. DOI:

10.1029/96JD00066.

- 537
538 (66) Bremer, H.; König, M. von; Kleinböhl, A.; Küllmann, H.; Künzi, K.; Bramstedt, K.; Burrows, J. P.;
539 Eichmann, K.-U.; Weber, M.; Goede, A. P. H. Ozone Depletion Observed by the Airborne
540 Submillimeter Radiometer (ASUR) during the Arctic Winter 1999/2000. *J. Geophys. Res. Atmos.*
541 **2002**, *107*, SOL 19-1-SOL 19-7. DOI: 10.1029/2001JD000546.
- 542 (67) Rex, M.; Salawitch, R. J.; Harris, N. R. P.; Gathen, P. von der; Braathen, G. O.; Schulz, A.;
543 Deckelmann, H.; Chipperfield, M.; Sinnhuber, B.-M.; Reimer, E.; Alfier, R.; Bevilacqua, R.; Hoppel,
544 K.; Fromm, M.; Lumpe, J.; Küllmann, H.; Kleinböhl, A.; Bremer, H.; König, M. von; Künzi, K.; Toohey,
545 D.; Vömel, H.; Richard, E.; Aikin, K.; Jost, H.; Greenblatt, J. B.; Loewenstein, M.; Podolske, J. R.;
546 Webster, C. R.; Flesch, G. J.; Scott, D. C.; Herman, R. L.; Elkins, J. W.; Ray, E. A.; Moore, F. L.; Hurst,
547 D. F.; Romashkin, P.; Toon, G. C.; Sen, B.; Margitan, J. J.; Wennberg, P.; Neuber, R.; Allart, M.;
548 Bojkov, B. R.; Claude, H.; Davies, J.; Davies, W.; Backer, H. De; Dier, H.; Dorokhov, V.; Fast, H.;
549 Kondo, Y.; Kyrö, E.; Litynska, Z.; Mikkelsen, I. S.; Molyneux, M. J.; Moran, E.; Nagai, T.; Nakane, H.;
550 Parrondo, C.; Ravegnani, F.; Skrivankova, P.; Viatte, P.; Yushkov, V. Chemical Depletion of Arctic
551 Ozone in Winter 1999/2000. *J. Geophys. Res. Atmos.* **2002**, *107*, SOL 18-1. DOI:
552 10.1029/2001JD000533.
- 553 (68) Jin, J. J.; Semeniuk, K.; Manney, G. L.; Jonsson, A. I.; Beagley, S. R.; McConnell, J. C.; Dufour, G.;
554 Nassar, R.; Boone, C. D.; Walker, K. A.; Bernath, P. F.; Rinsland, C. P. Severe Arctic Ozone Loss in
555 the Winter 2004/2005: Observations from ACE-FTS. *Geophys. Res. Lett.* **2006**, *33*, L15801. DOI:
556 10.1029/2006GL026752.
- 557 (69) Griffin, D.; Walker, K. A.; Wohltmann, I.; Dhomse, S. S.; Rex, M.; Chipperfield, M. P.; Feng, W.;
558 Manney, G. L.; Liu, J.; Tarasick, D. Stratospheric Ozone Loss in the Arctic Winters between 2005
559 and 2013 Derived with ACE-FTS Measurements. *Atmos. Chem. Phys.* **2019**, *19*, 577–601. DOI:
560 10.5194/ACP-19-577-2019.
- 561 (70) Feng, W.; Chipperfield, M. P.; Davies, S.; von der Gathen, P.; Kyrö, E.; Volk, C. M.; Ulanovsky, A.;
562 Belyaev, G. Large Chemical Ozone Loss in 2004/2005 Arctic Winter/Spring. *Geophys. Res. Lett.*
563 **2007**, *34*, L09803. DOI: 10.1029/2006GL029098.
- 564 (71) Zhang, J.; Tian, W.; Xie, F.; Chipperfield, M. P.; Feng, W.; Son, S.-W.; Abraham, N. L.; Archibald, A.
565 T.; Bekki, S.; Butchart, N.; Deushi, M.; Dhomse, S.; Han, Y.; Jöckel, P.; Kinnison, D.; Kirner, O.;
566 Michou, M.; Morgenstern, O.; O’Connor, F. M.; Pitari, G.; Plummer, D. A.; Revell, L. E.; Rozanov, E.;
567 Visioni, D.; Wang, W.; Zeng, G. Stratospheric Ozone Loss over the Eurasian Continent Induced by
568 the Polar Vortex Shift. *Nat. Commun.* **2018**, *9*, 206. DOI: 10.1038/s41467-017-02565-2.

569
570
571
572
573
574
575
576
577
578
579
580
581
582
583
584
585
586
587
588
589
590
591
592
593
594
595
596
597
598
599
600

- (72) Gelaro, R.; McCarty, W.; Suárez, M. J.; Todling, R.; Molod, A.; Takacs, L.; Randles, C. A.; Darmenov, A.; Bosilovich, M. G.; Reichle, R.; Wargan, K.; Coy, L.; Cullather, R.; Draper, C.; Akella, S.; Buchard, V.; Conaty, A.; Silva, A. M. da; Gu, W.; Kim, G.-K.; Koster, R.; Lucchesi, R.; Merkova, D.; Nielsen, J. E.; Partyka, G.; Pawson, S.; Putman, W.; Rienecker, M.; Schubert, S. D.; Sienkiewicz, M.; Zhao, B. The Modern-Era Retrospective Analysis for Research and Applications, Version 2 (MERRA-2). *J. Clim.* **2017**, *30*, 5419–5454. DOI: 10.1175/JCLI-D-16-0758.1.
- (73) McCormick, M. P.; Steele, H. M.; Hamill, P.; Chu, W. P.; Swissler, T. J. Polar Stratospheric Cloud Sightings by SAM II. *J. Atmos. Sci.* **1982**, *39*, 1387–1397. DOI: 10.1175/1520-0469(1982)039%3C1387:PSCSBS%3E2.0.CO;2
- (74) Varotsos, C. A.; Cracknell, A. P.; Tzanis, C. The Exceptional Ozone Depletion over the Arctic in January–March 2011. *Remote Sens. Lett.* **2011**, *3*, 343–352. DOI: 10.1080/01431161.2011.597792.
- (75) Dameris, M.; Loyola, D.; Nützel, M.; Coldewey-Egbers, M.; Lerot, C.; Romahn, F.; Van Roozendaal, M. Record Low Ozone Values over the Arctic in Boreal Spring 2020. *Atmos. Chem. Phys.* **2021**, *21*, 617–633. DOI: 10.5194/ACP-21-617-2021.
- (76) Alwarda, R.; Bognar, K.; Strong, K.; Chipperfield, M.; Dhomse, S.; Drummond, J.; Feng, W.; Fioletov, V.; Goutail, F.; Herrera, B.; Manney, G.; McCullough, E.; Millan, L.; Pazmino, A.; Walker, K.; Wizenberg, T.; Zhao, X. Record Springtime Stratospheric Ozone Depletion at 80°N in 2020. In *EGU General Assembly 2021, online, 19–30 Apr 2021*; 2021. DOI: 10.5194/egusphere-egu21-8892.
- (77) DeLand, M. T.; Bhartia, P. K.; Kramarova, N.; Chen, Z. OMPS LP Observations of PSC Variability During the NH 2019–2020 Season. *Geophys. Res. Lett.* **2020**, *47*, e2020GL090216. DOI: 10.1029/2020GL090216.
- (78) Curbelo, J.; Chen, G.; Mechoso, C. R. Lagrangian Analysis of the Northern Stratospheric Polar Vortex Split in April 2020. *Geophys. Res. Lett.* **2021**, *48*, e2021GL093874. DOI: 10.1029/2021GL093874.
- (79) Rao, J.; Garfinkel, C. I. Arctic Ozone Loss in March 2020 and Its Seasonal Prediction in CFSv2: A Comparative Study With the 1997 and 2011 Cases. *J. Geophys. Res. Atmos.* **2020**, *125*, e2020JD033524. DOI: 10.1029/2020JD033524.
- (80) Lee, S. H.; Lawrence, Z. D.; Butler, A. H.; Karpechko, A. Y. Seasonal Forecasts of the Exceptional Northern Hemisphere Winter of 2020. *Geophys. Res. Lett.* **2020**, *47*, e2020GL090328. DOI: 10.1029/2020GL090328.
- (81) Garfinkel, C. I.; Shaw, T. A.; Hartmann, D. L.; Waugh, D. W. Does the Holton–Tan Mechanism Explain How the Quasi-Biennial Oscillation Modulates the Arctic Polar Vortex? *J. Atmos. Sci.* **2012**,

601 69, 1713–1733. DOI: 10.1175/JAS-D-11-0209.1.

- 602 (82) Cohen, J.; Furtado, J. C.; Jones, J.; Barlow, M.; Whittleston, D.; Entekhabi, D. Linking Siberian Snow
603 Cover to Precursors of Stratospheric Variability. *J. Clim.* **2014**, *27*, 5422–5432. DOI: 10.1175/JCLI-D-
604 13-00779.1.
- 605 (83) Domeisen, D. I. V.; Garfinkel, C. I.; Butler, A. H. The Teleconnection of El Niño Southern Oscillation
606 to the Stratosphere. *Rev. Geophys.* **2019**, *57*, 5–47. DOI: 10.1029/2018RG000596.
- 607 (84) Holton, J. R.; Tan, H.-C. The Influence of the Equatorial Quasi-Biennial Oscillation on the Global
608 Circulation at 50 Mb. *J. Atmos. Sci.* **1980**, *37*, 2200–2208. DOI: 10.1175/1520-
609 0469(1980)037<2200:tioteq>2.0.co;2.
- 610 (85) Hurwitz, M. M.; Newman, P. A.; Garfinkel, C. I. The Arctic Vortex in March 2011: A Dynamical
611 Perspective. *Atmos. Chem. Phys.* **2011**, *11*, 11447–11453. DOI: 10.5194/ACP-11-11447-2011.
- 612 (86) Rao, J.; Ren, R.; Xia, X.; Shi, C.; Guo, D. Combined Impact of El Niño–Southern Oscillation and
613 Pacific Decadal Oscillation on the Northern Winter Stratosphere. *Atmosphere*. **2019**, *10*, 211. DOI:
614 10.3390/ATMOS10040211.
- 615 (87) Adams, C.; Strong, K.; Zhao, X.; Bassford, M. R.; Chipperfield, M. P.; Daffer, W.; Drummond, J. R.;
616 Farahani, E. E.; Feng, W.; Fraser, A.; Goutail, F.; Manney, G.; McLinden, C. A.; Pazmino, A.; Rex, M.;
617 Walker, K. A. Severe 2011 Ozone Depletion Assessed with 11 Years of Ozone, NO₂, and OClO
618 Measurements at 80N. *Geophys. Res. Lett.* **2012**, *39*, L05806. DOI: 10.1029/2011GL050478.
- 619 (88) Davies, S.; Chipperfield, M. P.; Carslaw, K. S.; Sinnhuber, B.-M.; Anderson, J. G.; Stimpfle, R. M.;
620 Wilmouth, D. M.; Fahey, D. W.; Popp, P. J.; Richard, E. C.; Gathen, P. von der; Jost, H.; Webster, C.
621 R. Modeling the Effect of Denitrification on Arctic Ozone Depletion during Winter 1999/2000. *J.*
622 *Geophys. Res. Atmos.* **2002**, *107*, SOL 65-1-SOL 65-18. DOI: 10.1029/2001JD000445.
- 623 (89) Arnone, E.; Castelli, E.; Papandrea, E.; Carlotti, M.; Dinelli, B. M. Extreme Ozone Depletion in the
624 2010-2011 Arctic Winter Stratosphere as Observed by MIPAS/ENVISAT Using a 2-D Tomographic
625 Approach. *Atmos. Chem. Phys.* **2012**, *12*, 9149–9165. DOI: 10.5194/ACP-12-9149-2012.
- 626 (90) Harris, N. R. P.; Rex, M.; Goutail, F.; Knudsen, B. M.; Manney, G. L.; Müller, R.; Gathen, P. von der.
627 Comparison of Empirically Derived Ozone Losses in the Arctic Vortex. *J. Geophys. Res. Atmos.*
628 **2002**, *107*, SOL 7-1-SOL 7-11. DOI: 10.1029/2001JD000482.
- 629 (91) Kuttippurath, J.; Goutail, F.; Pommereau, J. P.; Lefèvre, F.; Roscoe, H. K.; Pazmíno, A.; Feng, W.;
630 Chipperfield, M. P.; Godin-Beekmann, S. Estimation of Antarctic Ozone Loss from Ground-Based
631 Total Column Measurements. *Atmos. Chem. Phys.* **2010**, *10*, 6569–6581. DOI: 10.5194/ACP-10-
632 6569-2010.

633
634
635
636
637
638
639
640
641
642
643
644
645
646
647
648
649
650
651
652
653
654
655
656
657
658
659

660

661

(92) Chipperfield, M. P. Multiannual Simulations with a Three-Dimensional Chemical Transport Model. *J. Geophys. Res. Atmos.* **1999**, *104*, 1781–1805. DOI: 10.1029/98JD02597.

(93) Livesey, N. J.; Santee, M. L.; Manney, G. L. A Match-Based Approach to the Estimation of Polar Stratospheric Ozone Loss Using Aura Microwave Limb Sounder Observations. *Atmos. Chem. Phys.* **2015**, *15*, 9945–9963. DOI: 10.5194/ACP-15-9945-2015.

(94) Neale, R. E.; Barnes, P. W.; Robson, T. M.; Neale, P. J.; Williamson, C. E.; Zepp, R. G.; Wilson, S. R.; Madronich, S.; Andrady, A. L.; Heikkilä, A. M.; Bernhard, G. H.; Bais, A. F.; Aucamp, P. J.; Banaszak, A. T.; Bornman, J. F.; Bruckman, L. S.; Byrne, S. N.; Foereid, B.; Häder, D.-P.; Hollestein, L. M.; Hou, W.-C.; Hylander, S.; Jansen, M. A. K.; Klekociuk, A. R.; Liley, J. B.; Longstreth, J.; Lucas, R. M.; Martinez-Abaigar, J.; McNeill, K.; Olsen, C. M.; Pandey, K. K.; Rhodes, L. E.; Robinson, S. A.; Rose, K. C.; Schikowski, T.; Solomon, K. R.; Sulzberger, B.; Ukpebor, J. E.; Wang, Q.-W.; Wängberg, S.-Å.; White, C. C.; Yazar, S.; Young, A. R.; Young, P. J.; Zhu, L.; Zhu, M. Environmental Effects of Stratospheric Ozone Depletion, UV Radiation, and Interactions with Climate Change: UNEP Environmental Effects Assessment Panel, Update 2020. *Photochem. Photobiol. Sci.* **2021**, *20*, 1–67. DOI: 10.1007/S43630-020-00001-X.

(95) Bernhard, G. H.; Fioletov, V. E.; Grooß, J. U.; Ialongo, I.; Johnsen, B.; Lakkala, K.; Manney, G. L.; Müller, R.; Svendby, T. Record-Breaking Increases in Arctic Solar Ultraviolet Radiation Caused by Exceptionally Large Ozone Depletion in 2020. *Geophys. Res. Lett.* **2020**, *47*, e2020GL090844. DOI: [10.1029/2020GL090844](https://doi.org/10.1029/2020GL090844).

(96) Pommereau, J. P.; Goutail, F.; Pazmino, A.; Lefèvre, F.; Chipperfield, M. P.; Feng, W.; Van Roozendaal, M.; Jepsen, N.; Hansen, G.; Kivi, R.; Bognar, K.; Strong, K.; Walker, K.; Kuzmichev, A.; Khattatov, S.; Sitnikova, V. Recent Arctic Ozone Depletion: Is There an Impact of Climate Change? *Comptes Rendus - Geosci.* **2018**, *350* (7), 347–353. DOI: 10.1016/j.crte.2018.07.009.10.1016/j.crte.2018.07.009.

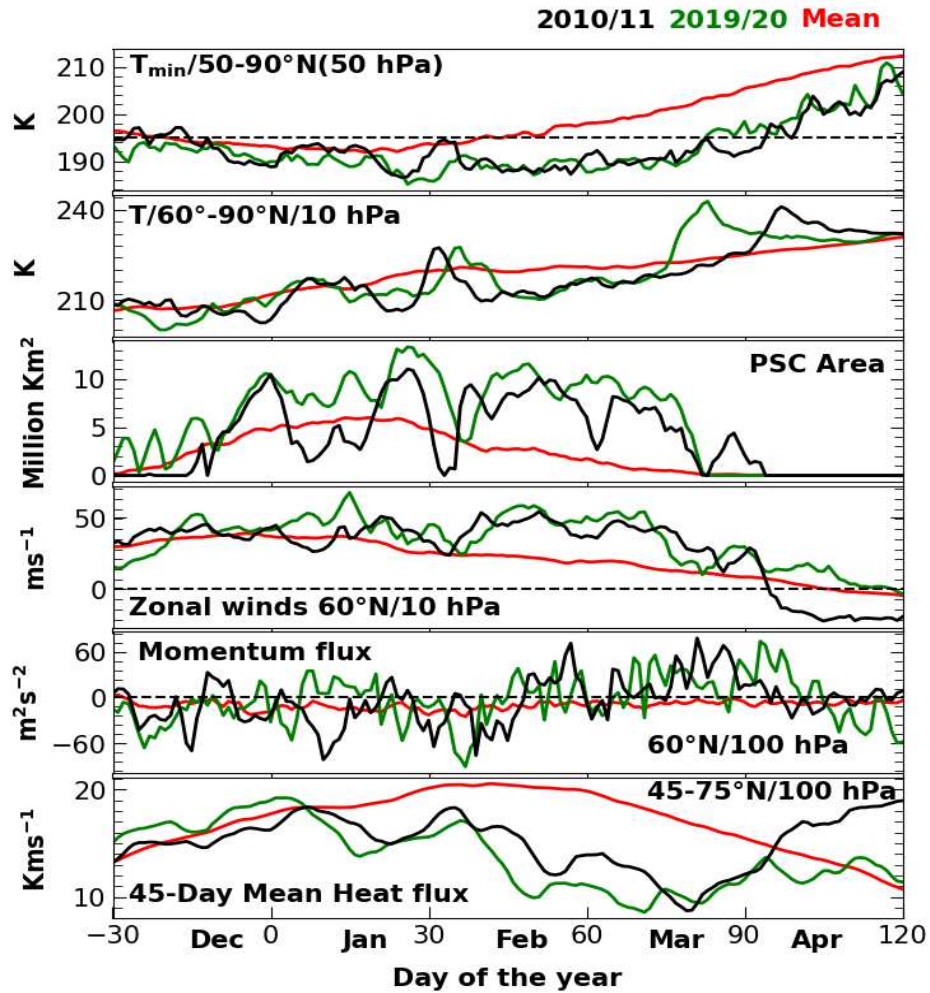
(97) Wilka, C.; Solomon, S.; Kinnison, D.; Tarasick, D. An Arctic Ozone Hole in 2020 If Not For the Montreal Protocol. *Atmos. Chem. Phys.* **2021**. DOI: [10.5194/acp-21-15771-2021](https://doi.org/10.5194/acp-21-15771-2021).

662 **Table 1:** Comparison of different parameters related to Arctic meteorology and chemistry during the
 663 winters 2011 and 2020.

Parameter	2011 Monthly Mean		2020 Monthly Mean	
	March	April	March	April
Minimum temperature (50 hPa)	191.29	198.74	190.54	202.5
60°–90°S Temperature (10 hPa)	213.22	217.14	215.31	215.48
PSC Area (460 K) (Million km ²)	5.0168	4.0466	7.1881	5.7600
PSC Volume (460 K) (Million km ³)	51.971	54.711	68.199	41.832
Total eddy heat flux (kms ⁻¹)	13.842	14.595	13.098	12.866
Vortex area (460 K) (Million km ²)	17.326	16.116	20.064	19.400
Vortex Edge Potential Vorticity (MPV) 1 PVU = 10 ⁻⁶ Kkg ⁻¹ m ² s ⁻¹	21.926	22.004	22.390	22.392
60°S zonal wind (10 hPa) (ms ⁻¹)	38.397	16.160	40.402	19.594
Momentum Flux at 60° (m ² s ²)	-5.6727	-4.6488	-4.4016	-3.1005
Wave 1 Amplitude of Geopotential Height at 60° (gpm)	198.19	186.40	196.53	202.75
Wave 2 Amplitude of Geopotential Height at 60° (gpm)	198.19	185.56	196.53	206.56
Ozone Minimum (DU)	248.65	250.06	238.31	238.22

664

665



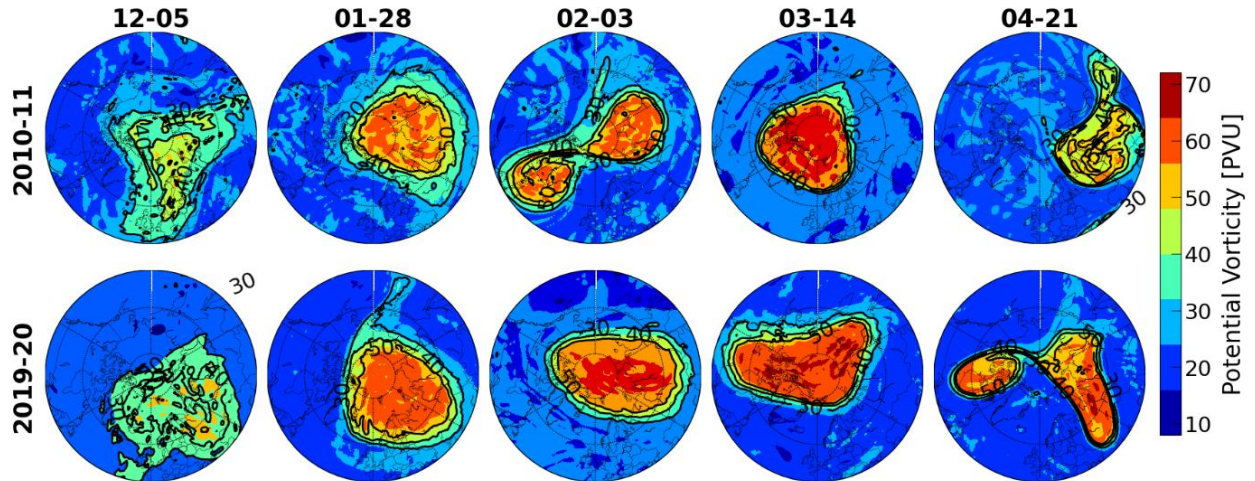
666 Figure 1: Meteorology of the winters. Seasonal evolution of the meteorological parameters during the
667 winters 2011 (black) and 2020 (green). The averaged meteorological parameters for the winters from
668 1979 to 2020 are also shown (red).

669

670

671

672



673

Figure 2: Temporal evolution of polar vortex. The position and strength of polar vortex in the Arctic

674

winters 2011 and 2020 as analyzed from the ERA5 data. The vortex situation in the lower stratosphere at

675

460 K (~16 km), the altitude of peak ozone loss, is illustrated.

676

677

678

679

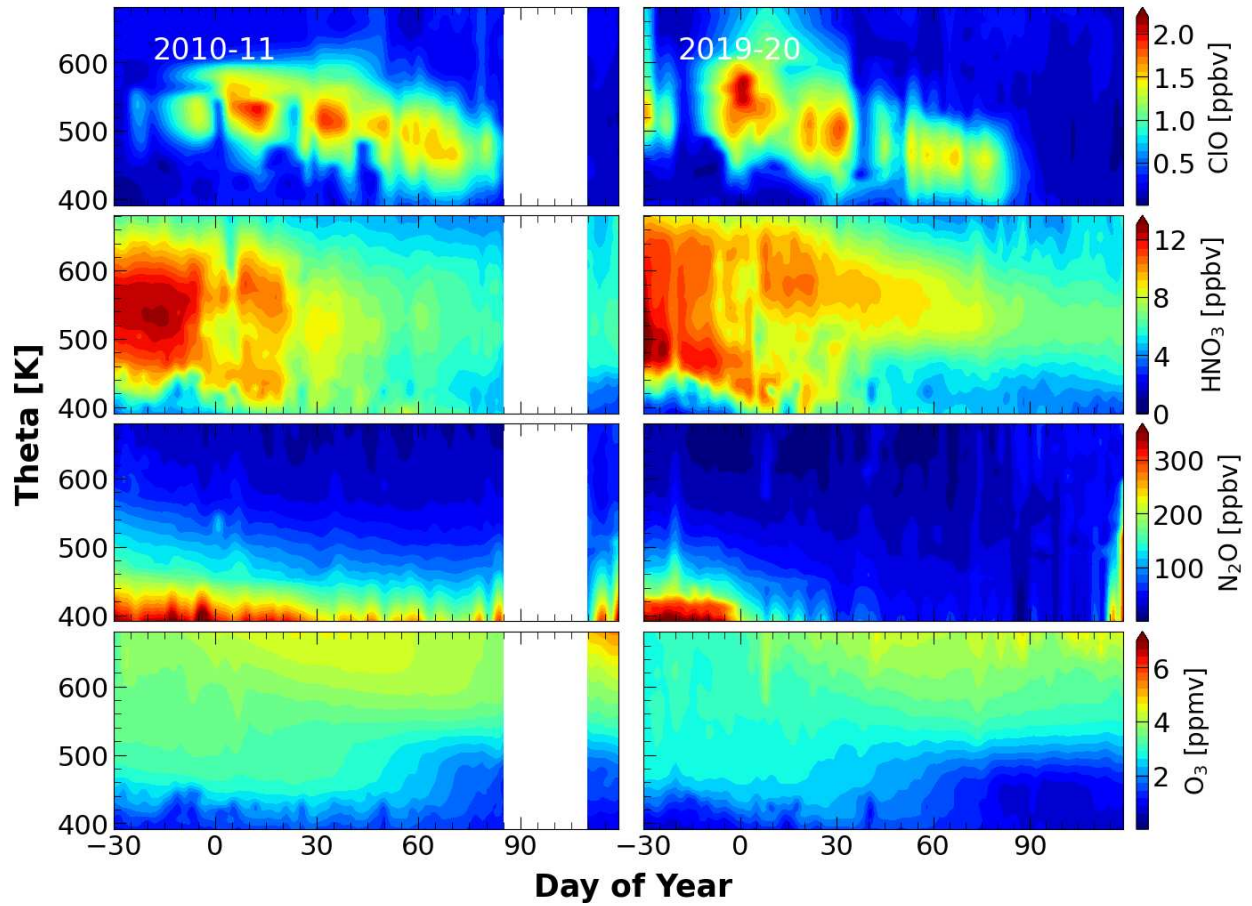
680

681

682

683

684



685 **Figure 3: Chemistry of the winters.** The distribution of ClO, HNO₃, N₂O, and ozone inside the polar vortex
686 for the Arctic during winter 2020 (right) and 2011 (left). The data shown are from the Microwave Limb
687 Sounder.

688

689

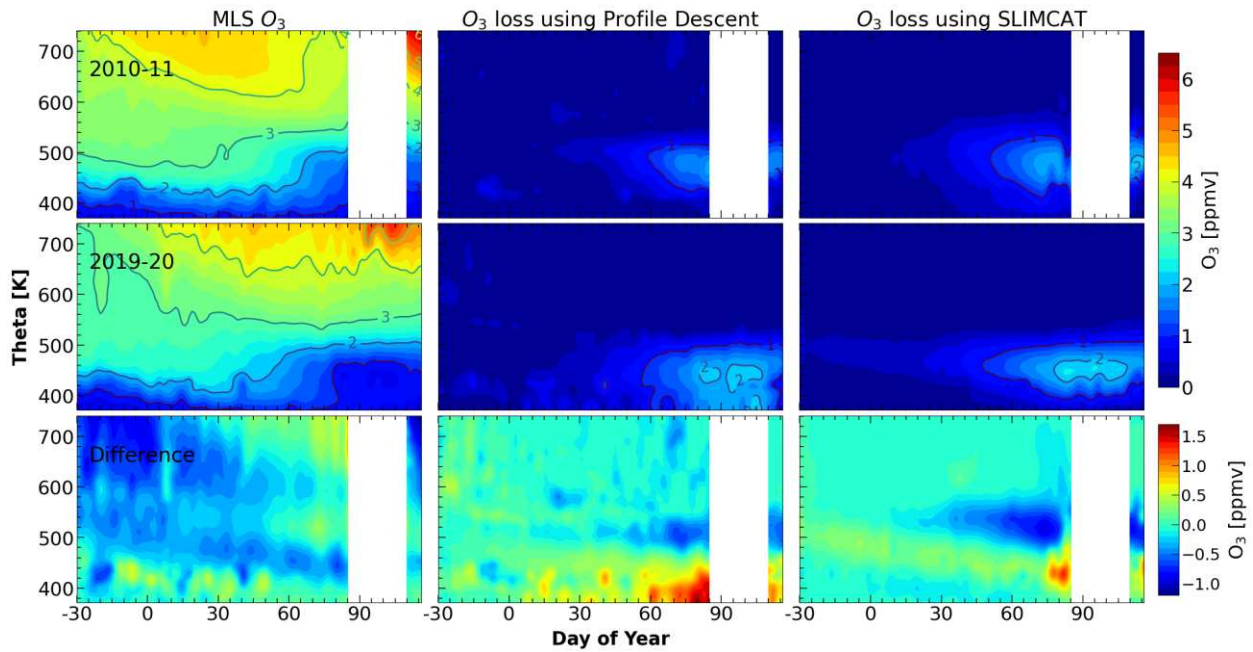
690

691

692

693

694

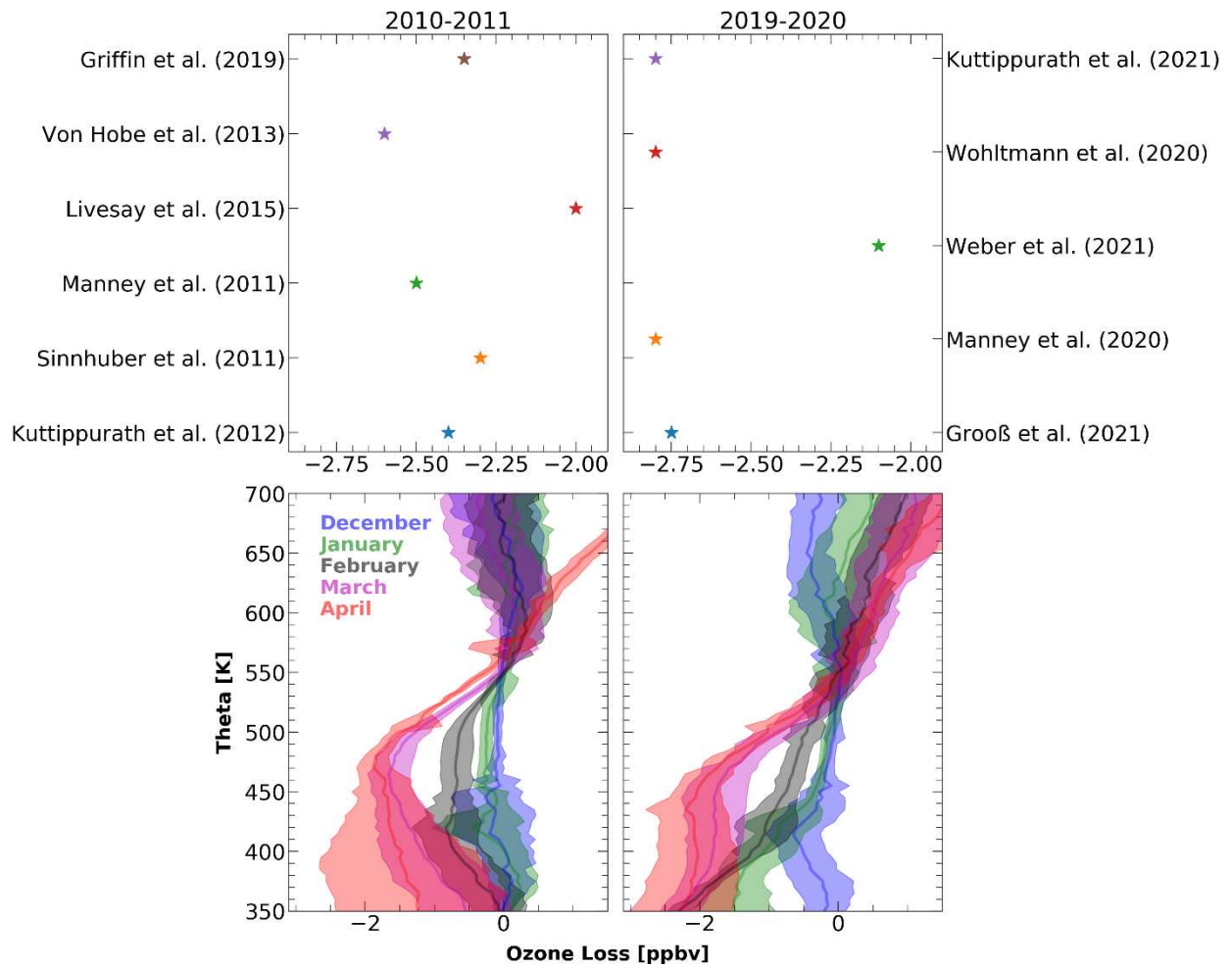


695 Figure 4: Ozone depletion in the Arctic winter 2011 and 2020. The ozone (left) ozone loss estimated using
696 the Microwave Limb Sounder measurements by applying the vortex descent (middle) method and passive
697 method (right) using the tracer simulations from SLIMCAT for the Arctic winters 2011 and 2020.

698

699

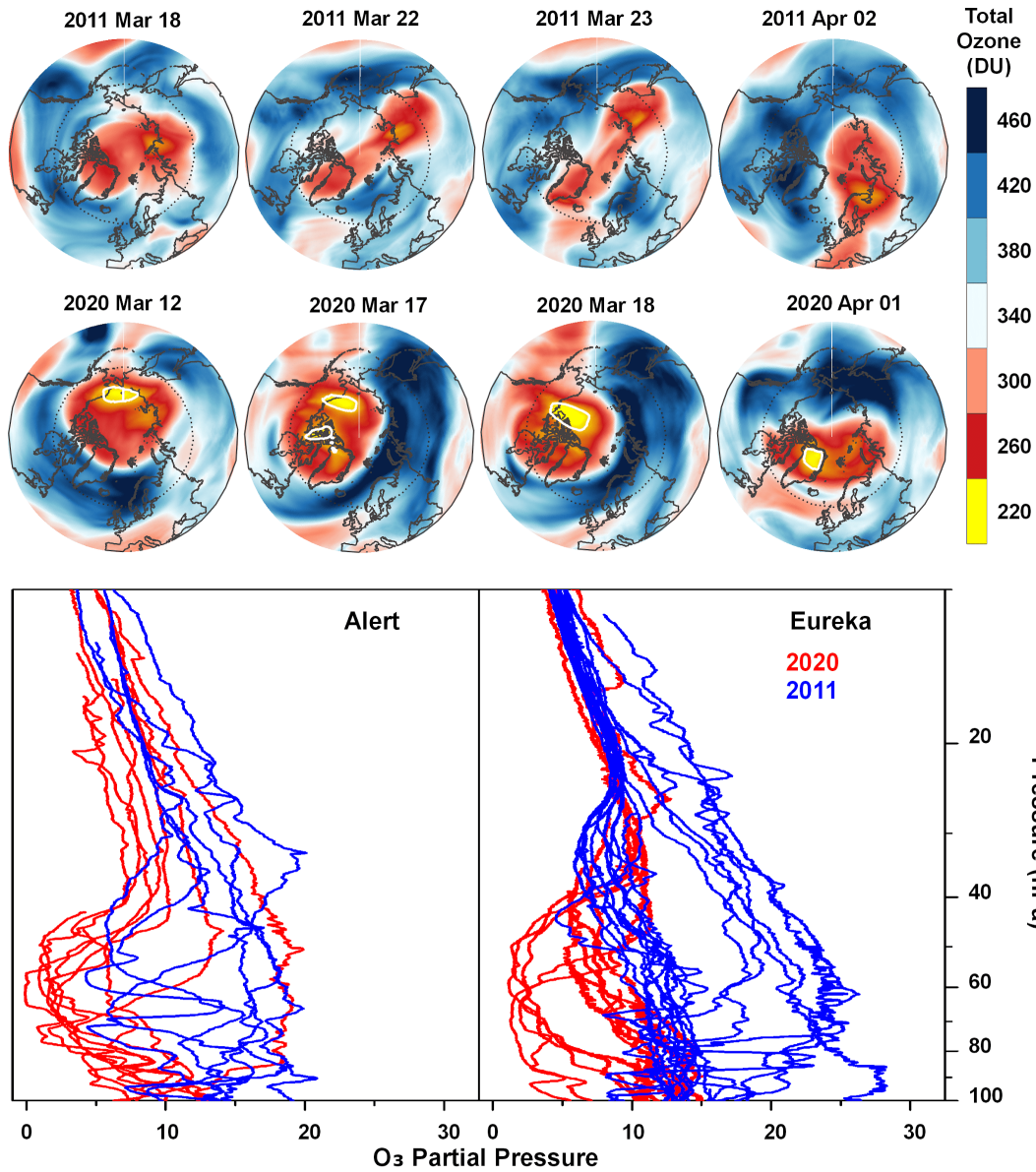
700



701 **Figure 5: Ozone loss in winter months.** The ozone loss estimated using the vortex descent method for each
702 winter and spring months in 2011 (left) and 2020 (left). The ozone loss estimated in different studies for
703 the winters 2011 and 2020 (upper panels).

704

705



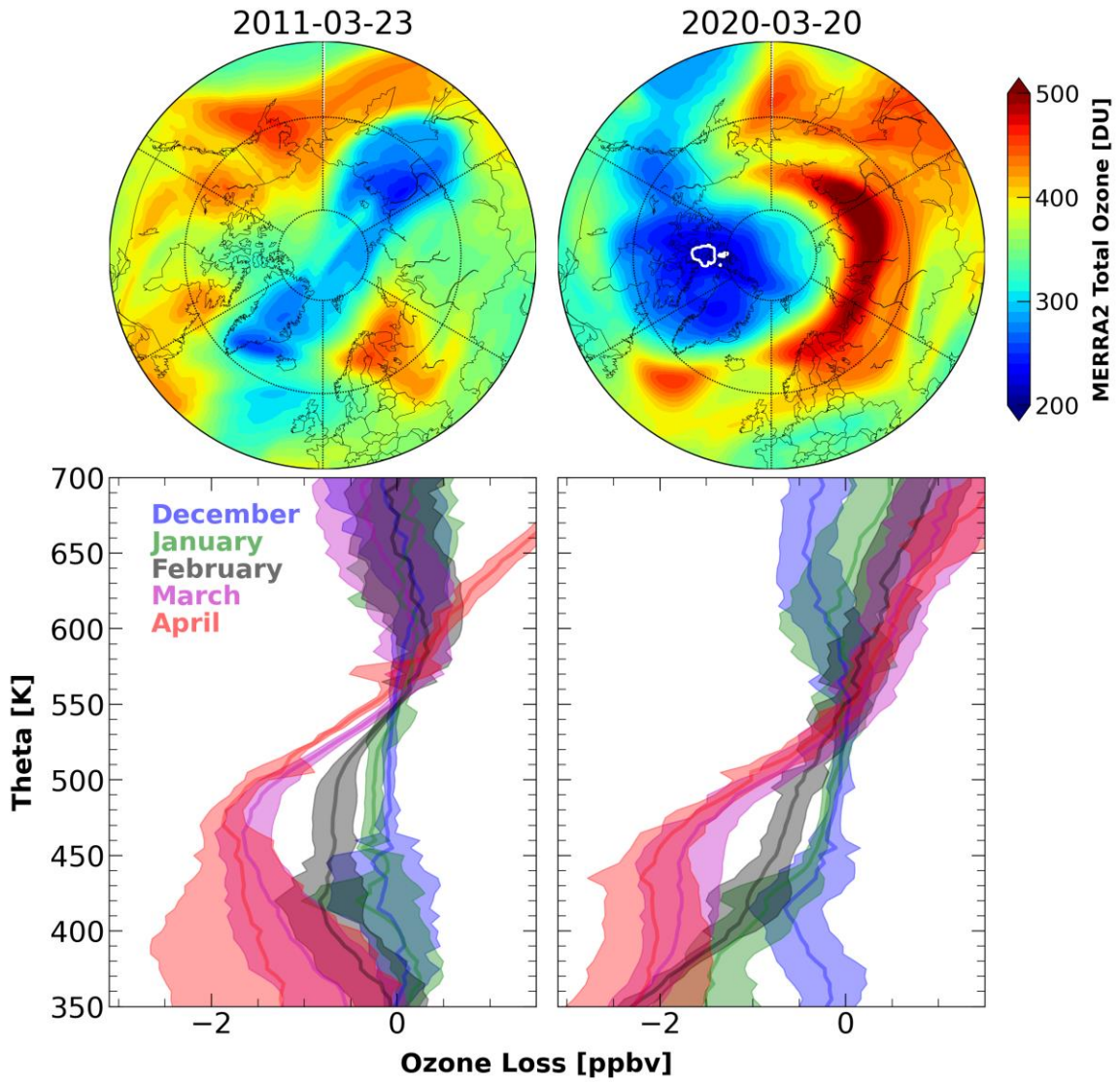
706 **Figure 6: Total column ozone and ozone loss saturation.** Total column ozone maps produced using MERRA-
707 2 data for the Arctic winters 2011 and 2020. The total ozone values below the ozone hole criterion (220
708 DU) are shown in yellow contours. The ozonesonde measurements were performed at two stations in the
709 Arctic (Eureka and Alert) during both winters (lower panels).

710
711
712

713 For TOC Only

714

715



716

717 JK/2REV/V02/08022022/11pm